cells

MDPI

Article

Temporal Transcriptomic Profiling of the Developing *Xenopus laevis* Eye

Samantha J. Hack [1], Juli Petereit [2] and Kelly Ai-Sun Tseng [3,*]

[1] Department of Biological Sciences, Western Michigan University, Kalamazoo, MI 49008, USA
[2] Nevada Bioinformatics Center, University of Nevada, Reno, NV 89557, USA
[3] School of Life Sciences, University of Nevada, Las Vegas, NV 89154, USA
* Correspondence: kelly.tseng@unlv.edu

Abstract: Retinal progenitor cells (RPCs) are a multipotent and highly proliferative population that give rise to all retinal cell types during organogenesis. Defining their molecular signature is a key step towards identifying suitable approaches to treat visual impairments. Here, we performed RNA sequencing of whole eyes from *Xenopus* at three embryonic stages and used differential expression analysis to define the transcriptomic profiles of optic tissues containing proliferating and differentiating RPCs during retinogenesis. Gene Ontology and KEGG pathway analyses showed that genes associated with developmental pathways (including Wnt and Hedgehog signaling) were upregulated during the period of active RPC proliferation in early retinal development (Nieuwkoop Faber st. 24 and 27). Developing eyes had dynamic expression profiles and shifted to enrichment for metabolic processes and phototransduction during RPC progeny specification and differentiation (st. 35). Furthermore, conserved adult eye regeneration genes were also expressed during early retinal development, including *sox2*, *pax6*, *nrl*, and Notch signaling components. The eye transcriptomic profiles presented here span RPC proliferation to retinogenesis and include regrowth-competent stages. Thus, our dataset provides a rich resource to uncover molecular regulators of RPC activity and will allow future studies to address regulators of RPC proliferation during eye repair and regrowth.

Keywords: eye development; retina; *Xenopus*; ocular transcriptome; retinal progenitor cells; cell signaling; Notch

Citation: Hack, S.J.; Petereit, J.; Tseng, K.A.-S. Temporal Transcriptomic Profiling of the Developing *Xenopus laevis* Eye. *Cells* **2024**, *13*, 1390. https://doi.org/10.3390/cells13161390

Academic Editors: Mehrnoosh Saghizadeh Ghiam and Vivien Coulson-Thomas

Received: 10 July 2024
Revised: 6 August 2024
Accepted: 14 August 2024
Published: 21 August 2024

1. Introduction

The incidence of preventable childhood blindness is falling; however, congenital causes of severe vision loss or impairment remain due to a lack of treatment options. Of specific therapeutic interest are retinal progenitor cells (RPCs), which are a multipotent population that give rise to all adult retinal cell types, including the retinal pigmented epithelium, photoreceptors, and retinal ganglion cells, as well as the Müller glia [1–3]. A first step towards generating new cell therapy and pharmacological treatment options is defining the molecular profile of developing optic tissues that contain cycling RPCs with the capacity to differentiate into appropriate cell types.

The African clawed frog, *Xenopus laevis* (*X. laevis*), is a powerful vertebrate system that has been used successfully for identifying the mechanisms that control normal and aberrant corneal, lens, and retinal development leading to visual impairments [4–6]. *X. laevis* is dually advantageous as a model system because it can also regenerate a variety of mature nervous tissues, including the retina, optic nerve, brain, and spinal cord [7]. It has recently been appreciated that midtailbud stage embryos are regrowth-competent and possess the ability to reform fully functional eyes following ablation [8,9]. Thus, *X. laevis* can be simultaneously used to investigate the similarities between developmental and regenerative transcriptional programs, as well as for identifying conserved vertebrate regulators of eye field development. This knowledge could allow researchers to address a

key question of whether/how regeneration recapitulates development—an important step in providing a solid basis for therapeutic designs for visual defects and injuries.

The *X. laevis* eye field is first specified in the anterior neural plate at developmental-stage (st.) 12.5/13 [10], where the overlapping expression of eye-field transcription factors (EFTFs) such as *pax6* in the eye primordium [11] specifies the RPCs committed to forming retinal tissues [12]. Retinal differentiation begins at st. 24 and is completed by st. 42, over a period of two days [3,13]. During early retinal development at st. 24, RPCs are mitotic, and less than 5% of RPCs have exited the cell cycle. By the mid to late retinal development periods (st. 29–38), RPCs that give rise to the presumptive ganglion cell layer (GCL) and ciliary marginal zone (CMZ) actively undergo differentiation [14–17]. Approximately 95% of RPCs exit the cell cycle by st. 37/38 [3], where progeny then continue to differentiate into the retinal cell types present in mature optic tissues. The developing lens arises from the invaginating lens placode, where the lens rudiment forms by st. 27 [4]. By st. 32, tissues become polarized into anterior and posterior domains, giving rise to the lens vesicle. Lens development is completed by st. 48 during the premetamorphic tadpole period [4].

In *Xenopus*, the early embryonic stages that include the specification of optic tissues have been extensively profiled by single-cell RNA sequencing, bulk RNA sequencing, and microarray experiments [18–22]. The larval and adult stages that include the mature eye have also been profiled [18]. These studies provide a rich resource for defining the molecular details of ocular tissue specification during embryogenesis and/or characterizing gene expression profiles of the mature eye. Additionally, pathways involved in retinal fate specification are well characterized [17,23–30]. However, retinal development begins in the early tailbud embryo at st. 24 [13]. As this key temporal window has not been characterized for *X. laevis* eye development, the specific molecular drivers of RPC proliferation and differentiation in developmental contexts remain unclear.

In this study, we utilize RNA sequencing (RNA-seq)to transcriptionally profile developing *X. laevis* eyes at three timepoints: from early tailbud stage embryos (st. 24, the beginning of retinal development), where approximately 95% of RPCs are mitotic [31]; at the mid tailbud stage (st. 27), where RPCs are regrowth-competent and remain highly proliferative; and during late retinal development (st. 35), where ~90% of RPCs have exited the cell cycle. Here, we generated a mineable resource to identify regulators of RPC activity and retinogenesis. Through differential expression (DE), Gene Ontology (GO), and KEGG pathway analyses, we show that the transcriptional environment is primed for retinogenesis between st. 24 and 27, where markers of early RPC proliferation are more highly expressed. Our analyses identify the st. 27 eye as highly dynamic; the gene expression profile exhibits characteristics and patterns observed at st. 24, but expression begins to shift from developmental signaling programs to enrichment for molecular programs associated with phototransduction and light perception. Moreover, we found that the Notch signaling pathway is highly enriched in st. 27 optic tissues, which is a regrowth-competent stage of eye development. Notch signaling components were among many conserved eye regeneration genes expressed in developing eyes across retinogenesis, further supporting a role for Notch signaling in the regulation of embryonic eye regrowth. Intriguingly, our transcriptional analysis also identified differential expression in long versus short gene homeologs across retinal development, suggesting that a detailed DE analysis examining all gene homeologs can identify novel roles for short versus long genes at different stages of embryogenesis.

2. Materials and Methods

2.1. Animal Care and Surgeries

Embryos were obtained via in vitro fertilization and cultured in 0.1× Marc's Modified Ringer (MMR: 1 mM $MgSO_4$, 2.0 mM KCl, 2 mM $CaCl_2$, 0.1 M NaCl, 5 mM HEPES, pH 7.8) medium [32]. Prior to eye ablation, st. 24, 27, and 35 embryos [33] were anesthetized with MS222 (MilliporeSigma, St. Louis, MO, USA). Fine surgical forceps (Dumont No. 5) were used to perform ablation surgery, as described previously [8,34]. For imaging, embryos

were fixed in MEMFA (100 mM MOPS (pH 7.4), 2 mM EGTA, 1 mM $MgSO_4$, and 3.7% formaldehyde) and washed with PBS + 0.1% Triton. Images were acquired using a Zeiss V20 Stereomicroscope with an Axiocam MRc camera.

2.2. Sample Collection and RNA Extraction

RNA samples were collected from *Xenopus laevis* embryos at three distinct developmental stages: 24, 27, and 35. Each stage was collected in triplicate (n = 3) and each biological replicate was composed of pooled eye tissues from 20 to 30 animals/embryos. Eye ablation and tissue dissociation were performed in Liberase (Thermolysin Medium Research Grade, Roche, Indianapolis, IN, USA) and/or calcium–magnesium-free Modified Ringer solution (CMF-MR) (adapted from [35]). Dissociated tissues were immediately stored in TRIzol Reagent (Invitrogen, Carlsbad, CA, USA) at −80 °C. Total RNA was isolated using the Direct-zol RNA Microprep Kit (Zymo Research, Irvine, CA, USA) according to the manufacturer's instructions.

2.3. Library Preparation and Sequencing

RNA-seq libraries were prepared from the extracted RNA using the Illumina TruSeq Stranded mRNA Library Prep Kit, utilizing 0.8 to 3.2 µg of input RNA. A diluted "A-Tailing Control" was introduced during ligation. Library quality was assessed using an Agilent Bioanalyzer and the molarity of the libraries was quantified using Roche KAPA qPCR. Paired-end sequencing with 150 cycles was performed on an Illumina NextSeq500 platform, and raw sequencing data were obtained from BaseSpace.

2.4. Data Preprocessing

Adapter contamination in the raw sequencing data was assessed and contamination levels below 0.1% were considered acceptable. Overrepresented sequences were identified and removed using Fastp v0.20. Pre-trimming reports were generated to assess pre- and post-trimming sequence quality.

2.5. Reference Genome and Annotation

The *Xenopus laevis* reference genome (XENLA_10.1_genome.fa) and annotation file (XENLA_10.1_GCF_XBmodels.gff3) were downloaded from Xenbase. The GFF3 annotation file was filtered to convert "pseudo" features to "exons" without gene IDs using the 'agat_sp_filter_feature_by_attribute_presence.pl' script. The filtered GFF3 file was then converted to GTF format using 'gffread' to facilitate compatibility with alignment tools such as STAR and HISAT.

2.6. Alignment, Quantification, and Quality Control Assessment

Trimmed RNA-seq data were aligned to the *Xenopus laevis* reference genome using both HISAT2 v2.2.1 and STAR v2.7 alignment tools. FeatureCounts was utilized to quantify reads assigned to genomic features. Quality control reports summarizing alignment statistics, read trimming data, and feature assignment were generated for both HISAT2 and STAR alignments. Comparisons between HISAT2 and STAR alignments were performed to assess alignment efficiency, with STAR demonstrating superior performance in terms of reads assigned to features.

2.7. RNA-seq Data Analysis

FeatureCounts data derived from the STAR alignment were imported into the statistical software R (v4.2 and above), where all downstream analyses were conducted. First, featureCounts underwent a quality control assessment to ensure sample quality and well-quantified transcripts. This included checking library sizes for consistency across all samples. Transcripts with at least 10 counts were considered well defined. To remove potential noise, a low count filter was applied, removing transcripts that (1) had too many zero counts across the samples and (2) had too many counts less than 10, as these could

be attributed to technical noise. Transcripts that were well defined in at least one of the three experimental groups were retained in the analysis. DESeq2 was used to process the filtered counts, and variance stabilization transformation (VST) data were used for all visualizations. Principal Component Analyses (PCA) were conducted on the raw, filtered, and transformed data to ensure data integrity. We conducted all pairwise comparisons to determine differential expression. Transcripts with a false discovery rate (FDR)-corrected value of less than 0.05 and an absolute value of log2 fold change of greater than or equal to 1 were deemed statistically significant and were used for Gene Ontology (GO) enrichment analysis and KEGG pathway analysis.

In addition to differential analysis, we further investigated the long (.L) and short (.S) versions of all transcripts. All transcripts with an L and S version were extracted. For each pair (e.g., lmo3.L and lmo3.S), we calculated the Spearman correlation (*rho*) and Euclidean distance (*d*) of the VST data to determine gene pairs with similar behavior or expression across developmental stages, respectively. We focused on three groups: (1) high differences in expression magnitudes ($d > 27$), (2) different expression patterns ($rho < -0.9$), and (3) we also extracted gene pairs of particular interest given prior knowledge to determine if their L and S versions demonstrated different expressions.

2.8. Enrichment Analysis

Gene expression data at different developmental stages (24, 27, and 35) of *X. laevis* were analyzed to identify differentially expressed genes (DEGs). DEGs were determined based on the criteria of an absolute log2 fold change threshold of 1 and an adjusted *p*-value of 0.05. Comparisons were made between consecutive developmental stages (27 vs. 24 and 35 vs. 27) to identify upregulated and downregulated genes. The Entrez IDs of well defined transcripts were annotated using the *X. laevis* annotation hub database (org.Xl.eg.db). Gene Ontology (GO) and Kyoto Encyclopedia of Genes and Genomes (KEGG) pathway enrichment analyses were conducted on the annotated genes using the enrichGO and enrichKEGG functions, respectively, from the clusterProfiler (v4.12) package in R. Both analyses applied a significance cutoff of 0.05. To refine the GO enrichment results and eliminate redundancy, the simplify function, also part of the clusterProfiler package, was utilized to remove redundant and higher-level GO IDs. All statistical analyses and enrichment analyses were performed in R. Figures summarizing the results of the differential expression analysis, as well as GO and KEGG enrichment analyses, were generated using the ggplot2 package in R.

3. Results and Discussion

3.1. Transcriptional Analysis of Developing Optic Tissues

To investigate the transcriptional changes in developing eyes across retinogenesis, we used previously published surgical procedures [9,34] to isolate whole optic tissues (including the overlying ectoderm, lens placode, and the optic vesicle; shown in Figure 1A,B) from *X. laevis* embryos at Nieuwkoop and Faber (NF) stages (st.) 24, 27, and 35 (Figure 1A) and conducted bulk RNA sequencing on poly-A-enriched mRNAs. Our transcriptional dataset spans from the early tailbud stage (st. 24 and 27), when the specification of retinal tissues begins in the developing optic vesicle, to retinal pigmented epithelium (RPE) morphogenesis and the formation of differentiated visual structures at st. 35, a late tailbud stage (Figure 1B). We previously showed that the transplantation of excised tissues to the trunk of the embryo is sufficient to form the major eye structures, including the lens, retina, and pigmented epithelium, ectopically [9]. Thus, using this tissue excision strategy, the transcriptional dataset can provide insight into the gene expression programs that give rise to several mature visual structures.

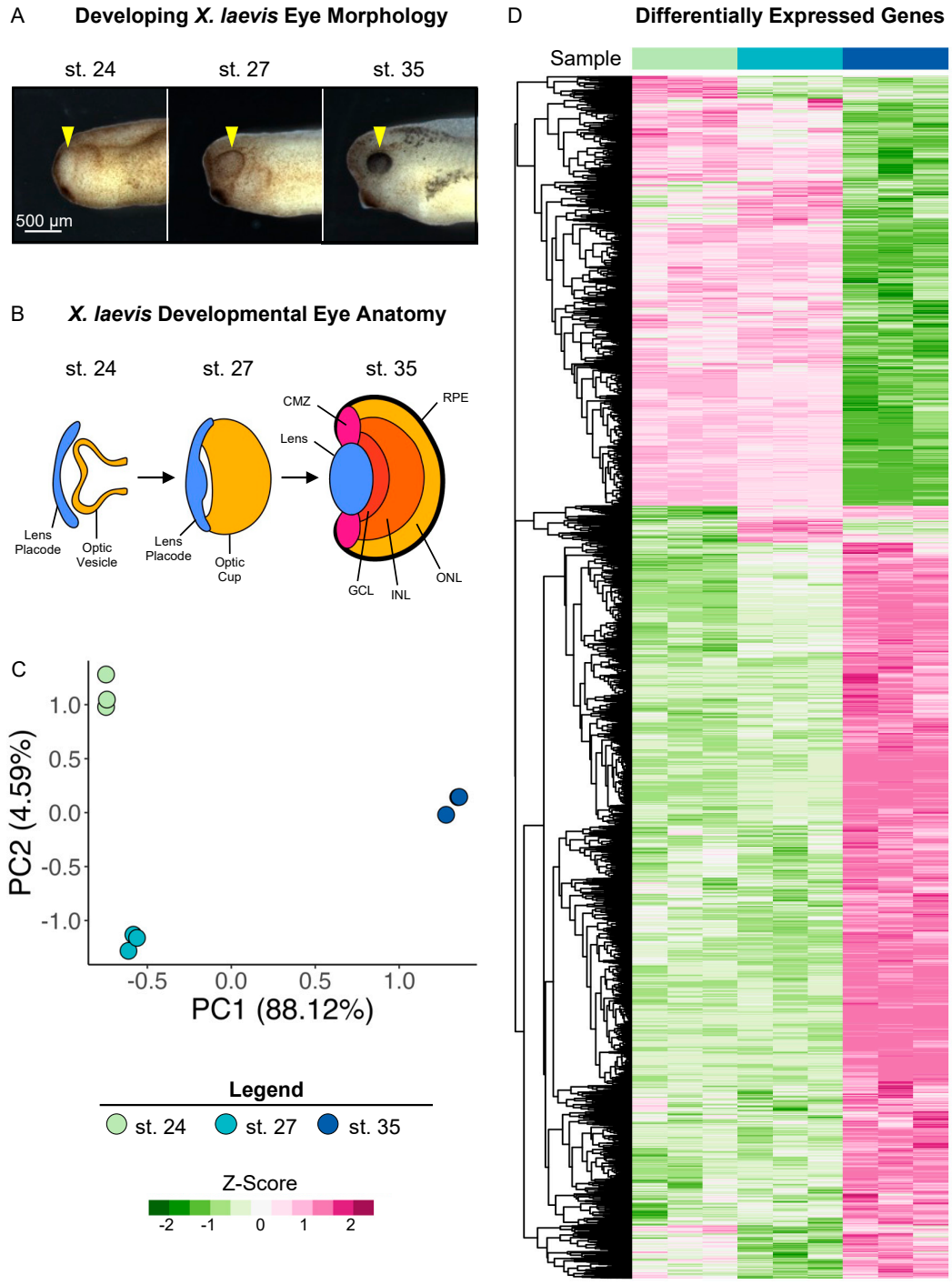

Figure 1. Transcriptional analysis of developing optic tissues. (**A**) *X. laevis* embryos at NF stages (st.) 24, 27, and 35, indicating the tissue that was resected for RNA sequencing and transcriptional analysis (yellow arrowhead). Scale bar: 500 µm. (**B**) Major optic structures present at each developmental stage assayed by RNA sequencing. CMZ: ciliary marginal zone; GCL: ganglion cell layer; INL: inner nuclear layer; ONL: outer nuclear layer; RPE: retinal pigmented epithelium. (**C**) Principal component analysis of whole transcriptome expression with triplicate samples for each developmental stage assayed. PC1: 88.12%, PC2: 4.95. (**D**) Relative expressions (Z-score vst counts) of statistically significantly differentially expressed genes between three developmental stages (st. 27 vs. 24 and st. 35 vs. 27). Rows are ordered by hierarchical clustering. Columns are ordered by stage.

Two major aligners, STAR and HISAT2, were used, and STAR showed a higher alignment rate than HISAT2 by assigning 200 k to 900 k more reads per sample. The overall assigned reads ranged from 19.9 to 25.6 million reads per sample (see Supplementary Table S1 for data quality control metrics). After the low count filter, the retained 17,693 transcripts were analyzed with the DESeq2 package. Of these, 3,746 genes did not have *Xenbase* IDs in the newest version of the genome (v10.1), and may thus represent novel transcripts (Supplementary Table S2). The principal component analysis (PCA) of the variance stabilizing transformed (vst) counts showed that developmental stages clustered in distinct groups. Transcriptional changes can be observed between all stages, with notable larger changes evidenced between st. 27 and 35 (Figure 1C).

We conducted differential expression analysis between the three developmental stages (st. 27 vs. st. 24 and st. 35 vs. st. 27) to identify specific patterns of differentially expressed genes (DEGs) over the period spanning early to late retinal development, as well as transcriptional similarities. Genes with an absolute value of $\log_2$ fold change ≥ 1 and FDR adj. $p < 0.05$ were deemed to be statistically significantly differentially expressed (Supplementary Table S2). We identified 1,126 (427 downregulated and 699 upregulated) and 8,403 (3074 downregulated and 5329 upregulated) DEGs by comparing st. 27 to 24 and st. 35 to 27, respectively. The PCA and differential expression analyses were well correlated, as expected; we predicted larger transcriptional changes at the later time point due to increased RPC differentiation and mature tissue formation (Figure 1A,D).

3.2. Eye Development Gene Expression across Retinogenesis

X. laevis is a well-established model of eye development, and numerous studies have described genes that have known mutant eye phenotypes. To determine if any of these known mutant genes were expressed in our transcriptional analyses, we mined the community resource *Xenbase* [36–38] for genes that produce phenotypes in the following categories when expression is manipulated: "Absence of eye," "Abnormal development of eye," "Decreased size of normal eye," and "Decreased size of eye primordium" (Supplementary Table S3). We queried the expression of 70 transcripts, and only 47 homeologs (67%) had detectable levels of expression after filtering for quantifiable counts (Figure 2A). By utilizing hierarchical clustering of the expressed transcripts, we identified a subset of known eye development genes expressed during early (st. 24 and st. 27) and late (st. 35) retinal development (Figure 2A). For example, the transcription factor *myc*, which is expressed in retinal stem cells located in the ciliary marginal zone (CMZ) [39], was upregulated at st. 27 compared to st. 35 (Figure 2A). A second cluster of development genes including *pitx3*, expressed during lens development [40], and *crx*, a transcriptional activator that regulates photoreceptor differentiation, were upregulated at st. 35 [41] (Figure 2A). We expected that genes associated with an absence of eye phenotypes would likely be expressed prior to eye differentiation; however, our results do not suggest a clear pattern between mutant eye phenotypes and the temporal expression of each gene at the timepoints we assessed. These data indicate that regulatory eye genes that are expressed during earlier developmental stages likely have diverse temporal expressions across development, and their function may differ depending on the context, i.e., the specification of the eye field or the completion of retinogenesis.

Figure 2. Expression of known vertebrate eye development genes. (**A**) Relative expression (Z-score vst counts) of genes with known eye development phenotypes in *X. laevis* at st. 24, 27, and 35. The phenotype associated with each gene (Xenbase [36–38]) is displayed to the left of each gene name. Multiple transcript variants of the same gene were included if applicable. (**B**) Relative expression (Z-score vst counts) of vertebrate eye development genes identified in *H. sapiens* and *M. musculus* at st. 24, 27, and 35. Multiple transcript variants of the same gene were included if applicable. Genes identified in the differential expression analysis (genes with FDR adj. $p < 0.05$ and absolute $\log_2$ fold change ≥ 1) between consecutive developmental stages are displayed to the left (purple: upregulated; green: downregulated; white: not differentially expressed).

Next, to investigate the extent to which the transcriptional regulation of retinal development may be conserved across species, we analyzed the expression of genes belonging to six molecular superclusters previously identified from RNA-seq analyses of the developing human retina [42] (Figure 2B). Two of these previously identified superclusters were associated with the positive regulation of proliferation and neural development; one supercluster showed the temporal upregulation of expression during early fetal retinogenesis (from embryonic days 52 to 57) and downregulated expression during later eye development stages [42]. Several genes belonging to these superclusters [42], including atonal homolog-7 (*atoh7*), fibroblast growth factor-19 (*fgf19)*, and cell cycle genes such as proliferating cell nuclear antigen (*pcna*) and cdk6, were also upregulated during early *Xenopus* retinal development between st. 24 and 27 in our own molecular analysis (Figure 2B). The four other superclusters identified in the molecular analysis of human retina development showed upregulated levels of expression during the late stages of retinogenesis (from embryonic day 125 to 136) [42]; these clusters were associated with biological processes such as synaptic transmission, phototransduction, and autophagy, among others [42]. Our results mirror this pattern, where the expression of genes from these superclusters tended to have increased expression levels at st. 35 (Figure 2B). For example, the glutamate receptor *grik-2*, neural retina leucine zipper (*nrl*), and acetylcholinesterase (*ache*) all had increased levels of expression at st. 35 compared to stgs. 24 and 27 (Figure 2B), which is similar to the temporal expression pattern observed for human fetal retinogenesis [42]. Interestingly, genes in an autophagy-associated supercluster that were upregulated in late fetal retinogenesis in humans [42], such as *sema-3b* (semaphorin-3b) and *plxna-1* (plexin-A1), were downregulated in st. 35 *Xenopus* eyes (Figure 2B). Collectively, our analysis of genes associated with human fetal retinal development suggests that the temporal expression of molecular signatures of early versus late retinogenesis may be conserved across vertebrate species.

Although there is heterogeneity in the RPC population at the same development stage, vertebrate RPCs have been classified into two groups based on conserved vertebrate transcriptional states identified from scRNA-seq studies [43]. "Primary RPCs" show an increased expression of cell cycle regulatory transcripts and are largely proliferative, whereas "neurogenic RPCs" express neural genes and undergo asymmetric cell division, where one daughter cell differentiates into a retinal cell [43]. We examined the conserved vertebrate gene markers that are characteristic of primary (proliferative) RPCs and neurogenic (differentiating) RPCs (Supplementary Table S4). Differentially expressed (FDR adj. $p < 0.05$, $\log_2$fold change ≥ 0.5) primary RPC markers were downregulated at st. 35 compared to st. 27. For example, the proliferative RPC marker *sfrp2.L* was significantly downregulated ($\log_2$fold change = -2.41) from st. 27 to st. 35, but was not differentially expressed between st. 24 and 27 (Supplementary Table S4). Conversely, 8/9 differentially expressed (FDR adj. $p < 0.05$, $\log_2$fold change ≥ 0.5) neurogenic RPC markers, including *rlbp1*, *car2*, and *crym*, were upregulated at st. 35 compared to st. 27 (Supplementary Table S4). The only downregulated neurogenic RPC marker at st. 35 was *sox8.S* ($\log_2$fold change = -0.87), which was previously shown to be expressed in cycling RPCs that give rise to Müller glia [44]. These data consistently show that RPCs in developing *X. laevis* eyes express conserved RPC markers in the temporal pattern observed in other vertebrate species, where primary RPC markers are more highly expressed during early retinogenesis (st. 24 and st. 27) and differentiating, neurogenic RPC markers are expressed during late retinogenesis (st. 35).

3.3. Gene Ontology (GO) Analysis of Developing Optic Tissues

To further explore temporal differences in the molecular profiles of developing optic tissues, we utilized Gene Ontology (GO) analysis [45] to uncover enriched biological processes and molecular functions in the DEGs identified between the three developmental stages (Figure 3). Biological processes involved in tissue development were enriched during early retinogenesis (st. 24 and st. 27), whereas GO terms associated with neuronal function and sensory perception were enriched during the later stage of eye formation

(st. 35) (Figure 3A). For example, we detected upregulation of 'retina development in camera-type eye', 'nervous system development', and 'cellular developmental process' at st. 27, whereas these biological processes were not enriched at st. 35 (Figure 3A). 'Neuron differentiation', 'visual perception', and 'neurotransmitter transport' were enriched at st. 35, in addition to several metabolic/biosynthetic processes (including lipid metabolism and ATP biosynthesis) (Figure 3A).

We detected similar patterns in molecular functions at each stage as well. Trends in GO term enrichment followed a pattern where eye development molecular programs are upregulated during early retinogenesis, while the transcriptional landscape begins moving towards upregulation of metabolic processes and neuronal activity associated with the acquisition of visual function during late retinogenesis (Figure 3B). For instance, GO terms like 'head development' and 'brain development' were downregulated at st. 27 compared to st. 24 (Figure 3B). Furthermore, 'photoreceptor activity' and 'calcium ion binding' were GO terms more highly enriched at st. 35 versus st. 27 (Figure 3B). Collectively, our analyses support previous work indicating that *X. laevis* eyes are largely differentiated by st. 35 and gain some initial function during the late tailbud-free swimming stages [46,47]. Moreover, these data suggest that st. 27 is a dynamic period in eye development, where molecular functions shift from RPC proliferation and retinogenesis to transcriptional programs associated with the differentiation of mature, functioning neurons.

3.4. KEGG Pathway Analyses Identify Hedgehog, PPAR, and Wnt Signaling as Potential Regulators of Eye Development

Similar to the GO analysis, we conducted Kyoto Encyclopedia of Genes and Genomes (KEGG) pathway analysis on the DEGs ($\log_2$ fold change ≥ 1 and FDR adj. $p < 0.05$) upregulated at both stages 24 and 27 during RPC proliferation and the DEGs upregulated at st. 35 (Figures 4 and S1) to highlight the molecular pathways that regulate retinogenesis. Consistent with the timing of active RPC proliferation, over 60 cell cycle-related genes were upregulated at the two early timepoints (st. 24 and 27). Our KEGG analyses indicated that canonical developmental pathways, including Wnt and Hedgehog signaling, were also upregulated at the early timepoints. This observation is consistent with previous studies, indicating that Wnt and Hedgehog signaling can regulate neural precursor proliferation [48–50] (Figure 4A). Hedgehog signaling is required for eye development in several models [51]. It has also been studied in the context of differentiation and the patterning of the eye, indicative of its multiple roles during retinogenesis (Figure 4A). Similarly, both canonical and non-canonical Wnt signaling are well-established regulators of vertebrate eye development, and mutations in pathway components result in eye abnormalities [52,53]. However, the requirement for signaling during different stages of eye development appears to be highly complex and species-dependent [53]. In *X. laevis*, *fzd-5* is required for RPC proliferation and retina development [54], but neurogenesis in the developing mouse retina is not dependent on *fzd-5* [55]. Given that Wnt signaling was also enriched at st. 27, it may play a role in regenerative neurogenesis as well. The role of Wnt signaling in embryonic eye regrowth is an exciting direction for future studies as it is a highly conserved regeneration signaling pathway [56].

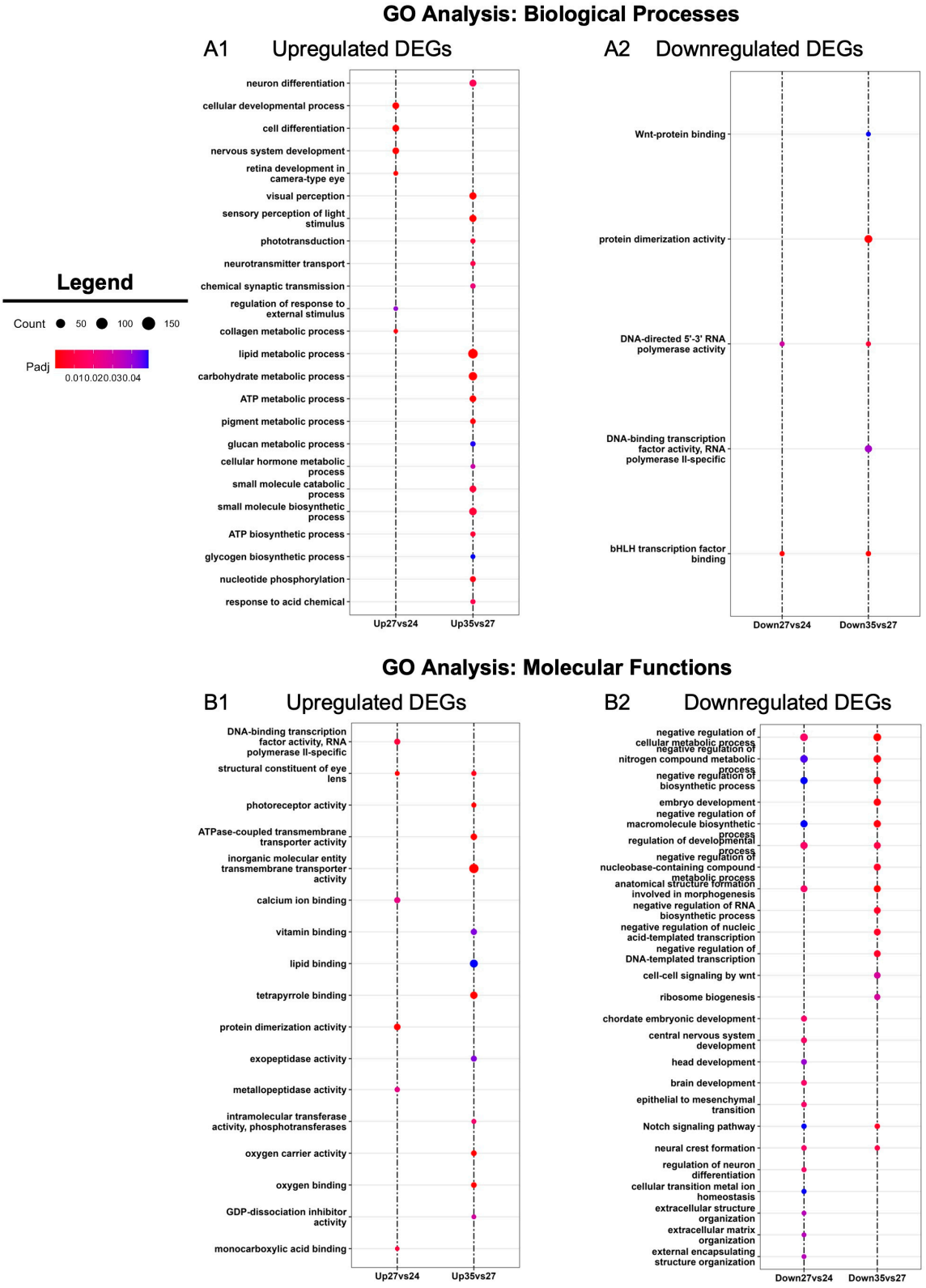

Figure 3. GO enrichment analysis. Gene Ontology (GO) analysis of statistically significantly differentially expressed genes (absolute $\log_2$ fold change ≥ 1 and FDR adj. $p < 0.05$) between consecutive developmental stages (st. 27 vs. 24 and st. 35 vs. 27). Enriched GO terms for (**A**) biological processes and (**B**) molecular functions.

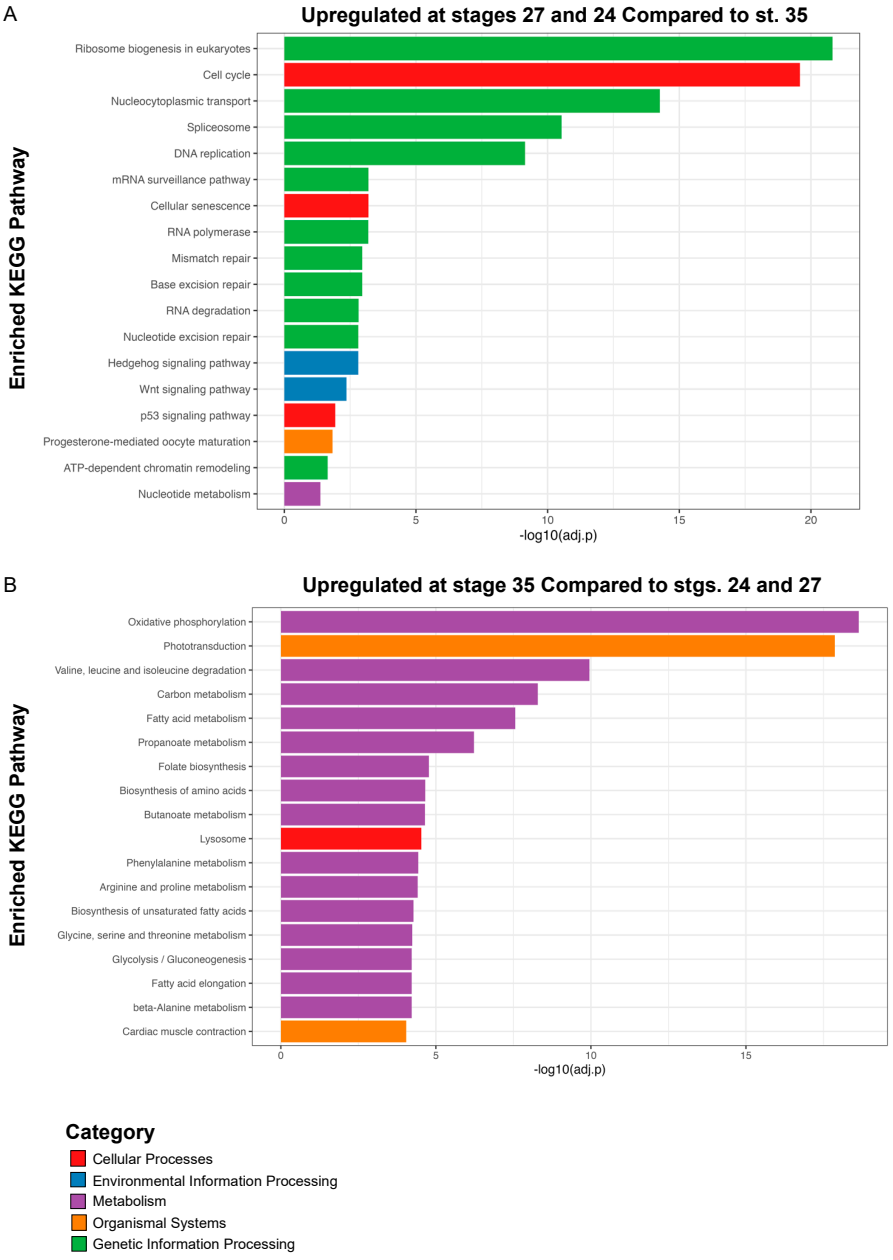

Figure 4. KEGG pathway enrichment analysis. Kyoto Encyclopedia of Genes and Genomes (KEGG) analysis of (**A**) statistically significantly upregulated genes at st. 24 and 27 compared to st. 35 and (**B**) statistically significantly upregulated genes at st. 35 compared to st. 24 and 27. Only top hits are shown in (**B**); for full list of KEGG pathways see Supplementary Figure S1.

In contrast to st. 24 and 27, we detected enrichment for a variety of metabolic and biosynthetic pathways in differentiating st. 35 optic tissues. Pathways associated with neuronal function such as "Phototransduction" and "Cardiac muscle contraction" were also highly enriched (Figure 4B). The full list of enriched pathways is shown in Figure S1. The mature retina is highly metabolically active [57]; thus, it was not unexpected that a number of biosynthetic pathways were upregulated during retinal differentiation. However, the spatiotemporal regulation of metabolism and molecular biosynthesis has not been well investigated in developing *Xenopus* nervous tissues. It was previously shown that a glycolysis gradient arises in the developing chick neural tube in response to the establishment of an FGF/Wnt signaling gradient; graded glycolytic activity is required for axis elongation and cell fate specification in the tail bud [58]. Similarly,

metabolic reprogramming during embryogenesis has been suggested as a mechanism to control stem cell differentiation and epigenetic states [59]. Our data suggest that metabolic reprogramming may occur during the late phase of retinal development, but whether this occurs in parallel with the onset of neuronal function or is associated with changes in the differentiation of RPCs and RPC progeny remains unclear and is a potential area of future investigation. Given that optic tissues have high metabolic demands [57] and that we detected enrichment for phototransductive pathways (Figure 4B), our KEGG analysis further suggests a switch to molecular programs associated with neuronal function during late retinal development.

3.5. Conserved Eye Regeneration Gene Expression Analysis across Retinal Development

Our recent work has shown that *X. laevis* eyes ablated at st. 27 are regrowth-competent and restore to age-appropriate size by 3 days post-surgery. Cell types are reborn in the order that parallels developmental retinogenesis [8,31,46]. Significantly increased levels of RPC proliferation during the first twenty-four hours post-injury facilitated regrowth and led to a temporal shift in retinogenesis not observed during normal development [8]. The developing eye transcriptome generated here temporally overlaps with regrowth-competent embryonic stages (from st. 24 to st. 28); our differential expression and GO analyses indicate that gene expression in optic tissues at st. 27 is highly dynamic. Plasticity in gene expression at this time may help to explain eye regrowth competency at this particular developmental stage. Given that the embryonic eye regrowth model was recently established and is distinct from well-studied models of adult eye regeneration in other model systems, such as *Danio rerio*, *Ambystoma mexicanum*, and *Schmidtea mediterranea,* we investigated if the *Xenopus* eye developmental transcriptional program has components shared with adult eye regeneration processes. We compiled a representative list of genes that are required for eye regrowth in these model systems and queried their expression in our dataset. Of the regeneration genes identified from the literature, most had increased expression levels at st. 24 and 27, whereas expression levels were reduced at st. 35 (Figure 5). However, a smaller subset of genes, including eye regeneration-associated orthodenticle homeobox transcription factors [60] (*otx-2*) and matrix metallopeptidase-9 (*mmp-9*) [61], had increased expression levels at st. 35 compared to st. 24 and 27 (Figure 5), suggesting that they are unlikely to play a role in embryonic eye regrowth.

The Notch signaling pathway is highly conserved across metazoans and plays essential roles in regulating proliferation, the specification of cell fate, and coordinating differentiation during embryonic development and during adult tissue homeostasis [62–64]. Furthermore, studies of Notch signaling in *Xenopus* have examined the role of Notch/Delta in earlier developmental stages (before st. 24) and the formation of the CMZ [65–69]. However, the role of Notch signaling during retinogenesis and the later stages of eye development in *Xenopus* remains unclear. Interestingly, the regeneration of diverse tissue types (including heart, liver, bone, and retina [70–73]) in many animal models also requires Notch signaling. Genes encoding core canonical Notch signaling components, including the receptor *notch-1* and target gene *hes-5*, were significantly upregulated at st. 27 compared to st. 24 or 35 (Figure 5), which was consistent with our KEGG pathway analysis showing the enrichment of Notch signaling specifically at st. 27 (FDR adj. $p = 1.75 \times 10^{-16}$). Importantly, our recent study showed that *notch-1* is required for RPC proliferation and embryonic eye regrowth in *X. laevis*, but was not required for the differentiation of regrowing optic tissues [74], supporting the analyses shown here. However, the potential mechanisms by which Notch signaling regulates embryonic eye regrowth remain unknown. Using our transcriptional analyses, we identified genes belonging to the canonical Notch pathway, known target genes of Notch signaling, and non-canonical Notch pathway components and visualized their relative expression across eye development at st. 24, 27, and 35 (Figure 6). Hierarchical clustering revealed that the temporal expression of noncanonical and canonical Notch pathway components may differ. Many target genes and canonical signaling components were significantly upregulated at st. 27, such as *hes5*, *dll1*, *notch.1* and *notch.3*, *adam.17*, and

dlc (Figure 6). This is similar to findings in mammalian models and zebrafish where cycling RPCs also show the expression of several *hes/her* genes [43,75–77]. Interestingly, many genes associated with noncanonical Notch signaling, such as Wnt ligands and SMAD genes, had higher relative expression at either st. 24 or st. 35 compared to st. 27 (Figure 6). Our data suggest that further investigation into the role of Notch signaling in both retinogenesis and embryonic eye regrowth may reveal molecular drivers of RPC proliferation.

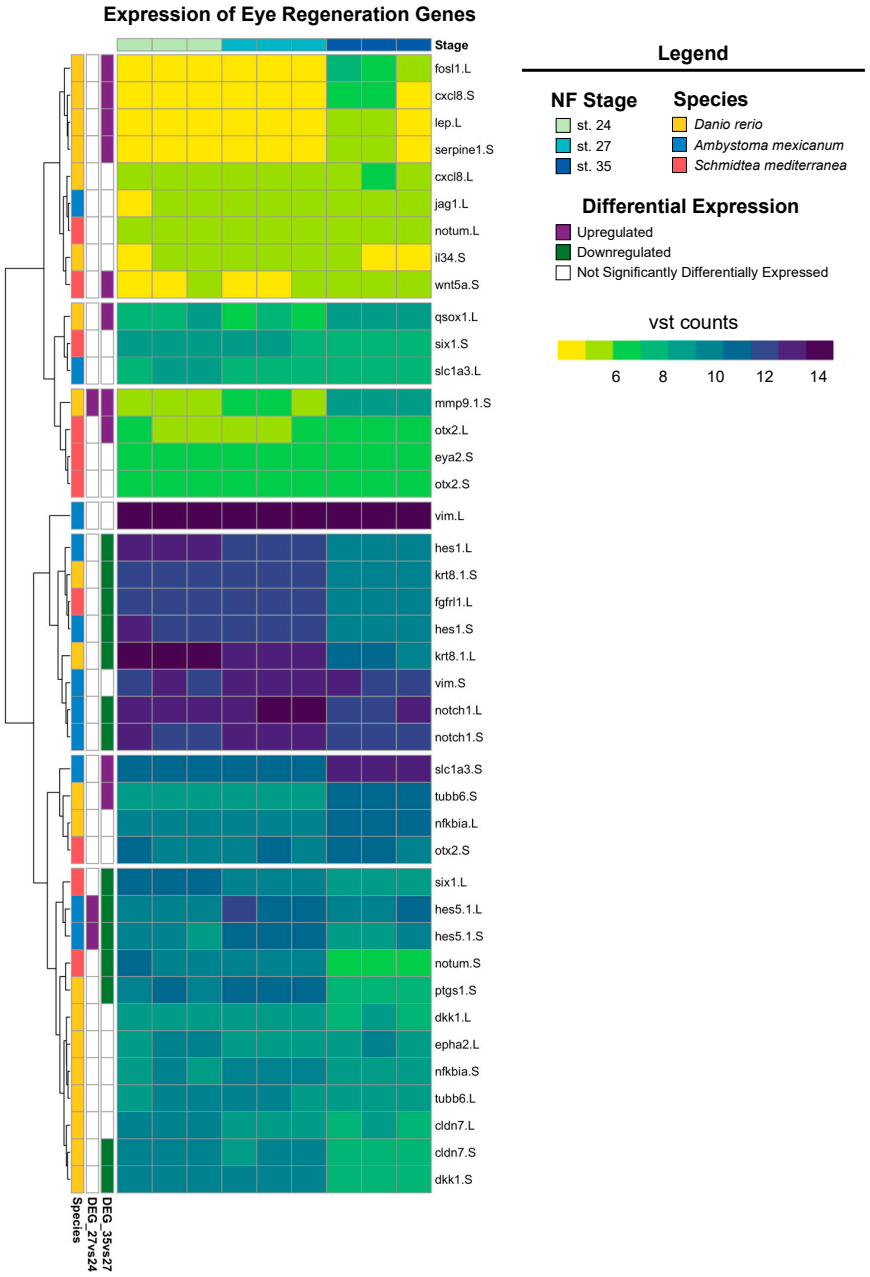

Figure 5. Expression of known eye regeneration genes. Expression (vst counts) of known eye regeneration genes in vertebrates (*D. rerio* and *A. mexicanum*) and the invertebrate *S. mediterranea* at st. 24, 27, and 35. Genes identified in the differential expression analysis (genes with FDR adj. $p < 0.05$ and absolute $\log_2$ fold change ≥ 1) between consecutive developmental stages are displayed to the left (purple: upregulated; green: downregulated; white: not differentially expressed).

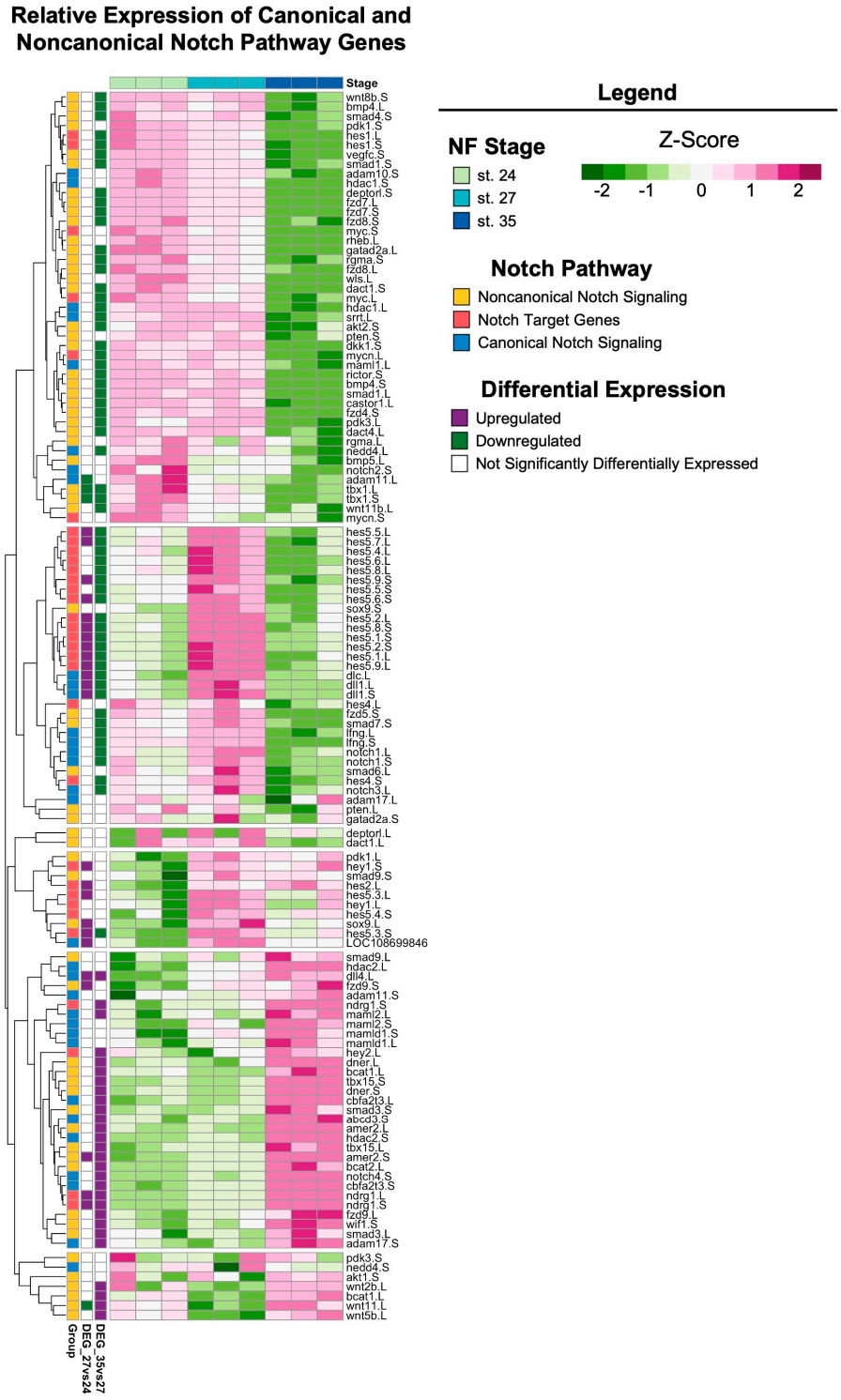

Figure 6. Notch signaling across retinal development. Relative expression (Z-score vst counts) of known Notch pathway genes (including genes that participate in canonical and noncanonical signaling, as well as downstream target genes) at st. 24, 27, and 35. Rows are ordered by hierarchical clustering and columns are ordered by stage. Genes identified in the differential expression analysis (genes with FDR adj. $p < 0.05$ and absolute $\log_2$ fold change ≥ 1) between consecutive developmental stages are displayed to the left (purple: upregulated; green: downregulated; white: not differentially expressed).

3.6. Long versus Short Gene Homeologs Are Differentially Expressed during Eye Development

X. laevis has an allotetraploid genome but is closely related to the diploid species *X. tropicalis*; it is hypothesized that two diploid species merged to form the allotetraploid 17–18 million years ago [78]. The two subgenomes, denoted as the Long (L) and Short (S), are characterized as having distinct classes of transposable elements, and while the subgenomes' structures have received recent attention, the molecular drivers of asymmetric subgenome evolution remain unclear [78]. Previous work has shown that homologous pairs of genes located in the L and S subgenomes have correlated expression levels, and most genes show slight expression bias towards the L homeolog [78,79]. However, a small subset of genes has a strong expression bias; the second copy (typically the S homeolog) has almost undetectable expression or has been lost from either subgenome entirely [79–81]. Since gene dosage and the optimization of gene expression are determinants of protein evolution, it is not surprising that gene loss or preferential retention is an important consequence of whole genome duplication [82,83]. Given that the L and S homeologs can be differentially expressed at unique developmental stages, we investigated whether retinal development follows the same patterns of *X. laevis* subgenome expression observed in other studies.

We identified 3,489 L and S homeologs within our dataset; their Spearman correlation ranged between −0.97 and 1 and the Euclidean distance ranged between 0.25 and 38.25. Most of them can be considered similar across developmental time given their high correlation and minimal distance (Figure 7A). Many genes from this subset, including *nrl*, *tbx1*, *sox-3*, *jund*, and *crybb1*, have known roles in eye development or embryogenesis more broadly [84–88]. A subset of genes also showed preferential expression of the L variant; 1,284 of 3,489 gene pairs (Figure 7B). Interestingly, some of these were categorized as ribosomal proteins, including *rps4, rps5, rps12, rps15, rpl6, rpl11, and eif3c* (Supplementary Table S5). Other groups of genes that displayed high variance between subgenome homeologs included chaperone proteins (*cct2* and *cct7*), genes associated with proliferation (*azin1*, *smc3*, *hmgb2*, *and ybx1*), and members of protein kinase C signaling (*rack1* and *kpna2*) (Supplementary Table S5).

Lastly, we identified several genes where the expression of L and S homeologs was negatively correlated across development (top hits shown in Figure 7C), and many of these displayed the preferential expression of the S homeolog at either st. 27 or st. 35. These included *endoul*, *atox1*, *nudt-5*, *ccnd-2,* and *uturn* (Figure 7D). For example, expression of the long and short homeologs of *endoul*, also known as placental protein 11 (*pp11*), were similar at st. 24 and 27, but *endoul.S* expression was highly upregulated at st. 35 (Figure 7D). Likewise, *nudt5.S* had elevated expression levels compared to *nudt5.L* at st. 35 (Figure 7D). Other genes like *atox1.S* and *utrn.S* had higher expression levels at all stages compared to the long homeolog of each gene (Figure 7D); *utrn.S* had an upregulated expression specifically at st. 27 (Figure 7D). The identification of significant differences in the transcriptional profiles of developmentally relevant genes, including *endoul*, suggests that L and S subgenomes may differentially contribute to different retinal developmental processes. While subgenome-specific mutations may have arisen in many genes, it is currently unclear why some homeologs are preferentially expressed when their sequence or protein domains are conserved between subgenomes. Given the L subgenome is typically used for the analysis of RNA-seq datasets, our findings highlight that the analysis of both L and S homeologs is an important step for identifying candidate genes during differential expression analysis. Lastly, it is now appreciated that the L subgenome developed after the S subgenome, and that many genes have been lost from S [78]. It will be interesting to consider how the evolution of allotetraploid subgenomes may have driven the development of regenerative abilities or species-specific metamorphic processes, or whether the retention of expression from S homeologs confers advantages during distinct developmental stages.

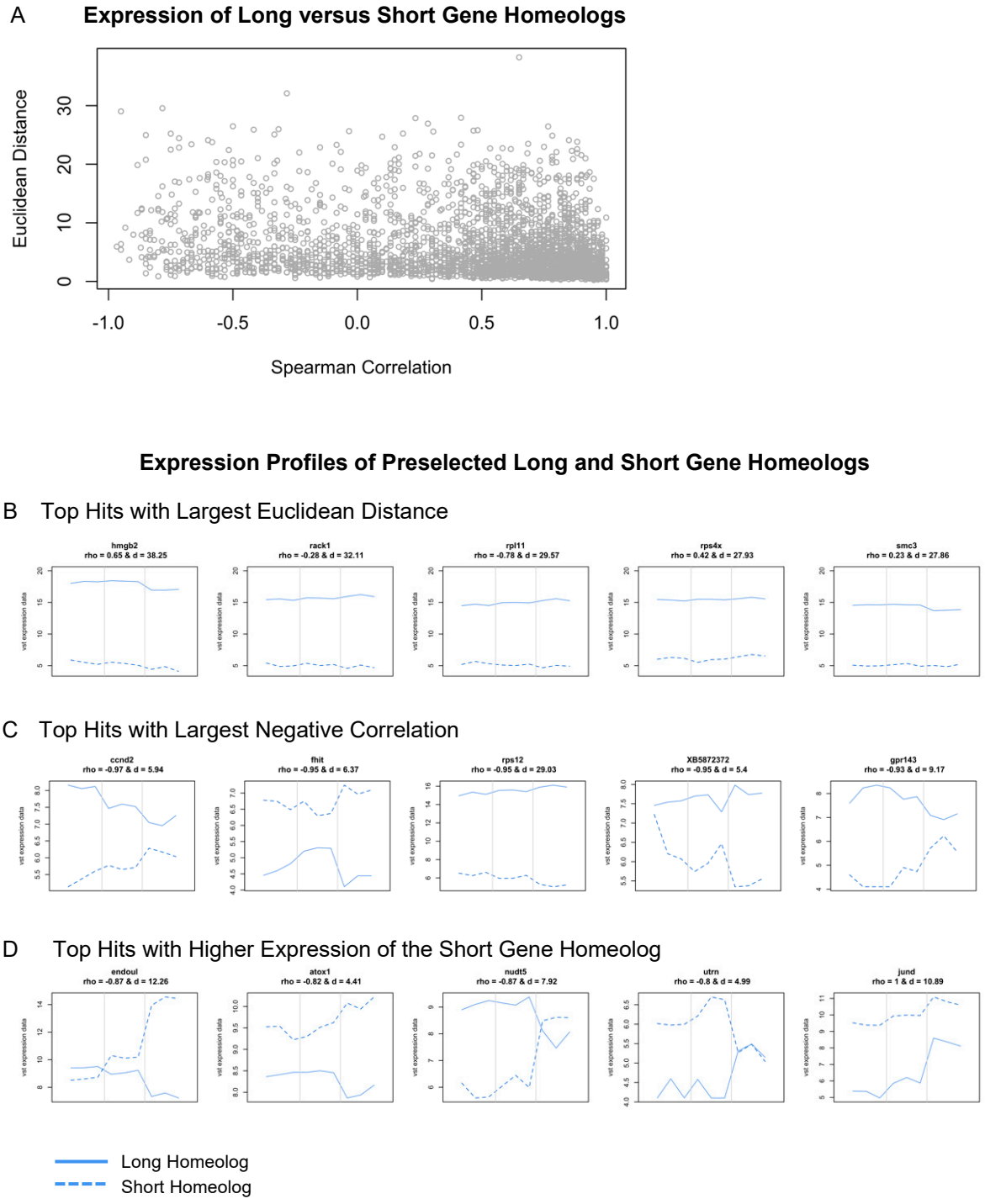

Figure 7. Expression analysis of long and short gene homeologs across retinal development. (**A**) Scatterplot of Spearman's correlation coefficient versus the Euclidean distance of L and S homeologs. (**B**–**D**) Expression profiles (vst counts) of selected hits identified in (**A**). Homeologs with (**B**) largest Euclidean distance (the largest expression difference across developmental stages), (**C**) highest negative correlation (behaving most differently across developmental stages), and (**D**) short gene homeologs with higher expression than their long homeolog. Dashed lines: Expression of the short homeolog. Solid lines: Expression of the long homeolog. The Spearman's correlation coefficient (*rho*) and Euclidean distance (*d*) for homeologs are displayed at the top of the corresponding expression profiles.

4. Conclusions

A first step towards generating therapeutics to treat ocular diseases is improving our understanding of the molecular drivers of eye development and successful repair. Here, we used RNA sequencing to define the temporal transcriptomes of the *X. laevis* eye across three distinct developmental stages that span the early retinal development period of active RPC proliferation (st. 24 and 27) and then retinogenesis (st. 35). The identification of DEGs during retinal developmental stages coupled with GO and KEGG enrichment analyses indicated that the eye transcriptome between st. 24 and st. 35 is highly dynamic. Importantly, the tissues used for analysis included RPCs that must proliferate and differentiate properly to form the neural retina and RPE. Thus, future single-cell studies coupled with this bulk transcriptional analysis may uncover drivers of RPC proliferation and markers of retinal stem cells. Furthermore, we show that st. 27 optic tissues, which are regrowth-competent, express known markers of adult eye regeneration observed in other species. Specifically, Notch signaling was enriched at a regrowth-competent stage, indicating that this key pathway may regulate RPC proliferation and maintenance during both development and regeneration. We also uncovered unique and variable expression profiles between long and short gene homeologs during retinal development. Our data indicated that an examination of both subgenomes for bioinformatic analysis is crucial for identifying potential molecular differences between the expression of long and short gene homeologs during different biological processes. Lastly, this study shows that *X. laevis* RPC transcriptomes are consistent with the RPC marker expression patterns observed in mammalian models. This essential knowledge, combined with the distinct ability of *Xenopus* RPCs to endogenously restore the embryonic eye after injury, can facilitate ongoing investigations pinpointing potential eye repair strategies.

Supplementary Materials: The following supporting information can be downloaded at: https://www.mdpi.com/article/10.3390/cells13161390/s1, Figure S1: All enriched KEGG pathways at st. 35; Table S1: MultiQC v1.12 general statistics, Table S2: STAR aligned transcripts following DESeq2 analysis, Table S3: Expression of known *Xenopus* eye development genes, Table S4: Expression of known retinal progenitor cell (RPC) markers, Table S5: Long versus short homeolog expression.

Author Contributions: Conceptualization, K.A.-S.T.; formal analysis, S.J.H. and J.P.; investigation, S.J.H., J.P., and K.A.-S.T.; resources, J.P. and K.A.-S.T.; data curation, J.P.; writing—original draft preparation, S.J.H.; writing—review and editing, S.J.H., J.P. and K.A.-S.T.; visualization, J.P. and S.J.H.; supervision and project administration, K.A.-S.T.; funding acquisition, S.J.H., J.P. and K.A.-S.T. All authors have read and agreed to the published version of the manuscript.

Funding: This study was supported by grants from the National Institutes of Health (GM146672, GM103440, and U54 GM104944). This work was also supported by a Western Michigan University Dissertation Completion Fellowship to S.J.H.

Institutional Review Board Statement: Adult *Xenopus laevis* were purchased from Nasco (Janesville, WI, USA) and grown via approved protocols and guidelines (University of Nevada, Las Vegas Institutional Animal Care and Use Committee).

Informed Consent Statement: Not applicable.

Data Availability Statement: Raw sequencing data have been deposited to the Sequence Read Archive (SRA) as part of https://www.ncbi.nlm.nih.gov/ and are accessible under accession number PRJNA1124041. Other relevant data supporting the key findings of this study are available within the article, supplementary information, public repositories, or from the corresponding author upon reasonable request. Correspondence and material requests should be sent to Kelly Tseng.

Acknowledgments: We thank Cindy Kha for tissue dissections and RNA isolation, the Nevada Genomics Center (Paul Hartley) for sequencing the samples, and the Nevada Bioinformatics Center (RRID:SCR_017802) (Lucas Bishop, Jeremiah B. Reyes, Hans Vasquez-Gross, and Richard Tillett) for bioinformatics support. We also thank Wendy Beane for comments and the Xenbase team for help with annotations.

Conflicts of Interest: All authors declare no competing interests.

References

1. Wetts, R.; Fraser, S.E. Multipotent precursors can give rise to all major cell types of the frog retina. *Science* **1988**, *239*, 1142–1145. [CrossRef] [PubMed]
2. Turner, D.L.; Cepko, C.L. A common progenitor for neurons and glia persists in rat retina late in development. *Nature* **1987**, *328*, 131–136. [CrossRef]
3. Holt, C.E.; Bertsch, T.W.; Ellis, H.M.; Harris, W.A. Cellular determination in the Xenopus retina is independent of lineage and birth date. *Neuron* **1988**, *1*, 15–26. [CrossRef] [PubMed]
4. Viet, J.; Reboutier, D.; Hardy, S.; Lachke, S.A.; Paillard, L.; Gautier-Courteille, C. Modeling ocular lens disease in Xenopus. *Dev. Dyn.* **2020**, *249*, 610–621. [CrossRef]
5. Pratt, K.G.; Khakhalin, A.S. Modeling human neurodevelopmental disorders in the *Xenopus* tadpole: From mechanisms to therapeutic targets. *Dis. Model. Mech.* **2013**, *6*, 1057–1065. [CrossRef]
6. Nakayama, T.; Fisher, M.; Nakajima, K.; Odeleye, A.O.; Zimmerman, K.B.; Fish, M.B.; Yaoita, Y.; Chojnowski, J.L.; Lauderdale, J.D.; Netland, P.A.; et al. *Xenopus pax6* mutants affect eye development and other organ systems, and have phenotypic similarities to human aniridia patients. *Dev. Biol.* **2015**, *408*, 328–344. [CrossRef] [PubMed]
7. Lee-Liu, D.; Méndez-Olivos, E.E.; Muñoz, R.; Larraín, J. The African clawed frog *Xenopus laevis*: A model organism to study regeneration of the central nervous system. *Neurosci. Lett.* **2017**, *652*, 82–93. [CrossRef]
8. Kha, C.X.; Son, P.H.; Lauper, J.; Tseng, K.A. A model for investigating developmental eye repair in *Xenopus laevis*. *Exp. Eye Res.* **2018**, *169*, 38–47. [CrossRef] [PubMed]
9. Kha, C.X.; Guerin, D.J.; Tseng, K.A. Using the *Xenopus* Developmental Eye Regrowth System to Distinguish the Role of Developmental Versus Regenerative Mechanisms. *Front. Physiol.* **2019**, *10*, 502. [CrossRef]
10. Zuber, M.E. Eye field specification in *Xenopus laevis*. *Curr. Top. Dev. Biol.* **2010**, *93*, 29–60. [CrossRef]
11. Zuber, M.E.; Gestri, G.; Viczian, A.S.; Barsacchi, G.; Harris, W.A. Specification of the vertebrate eye by a network of eye field transcription factors. *Development* **2003**, *130*, 5155–5167. [CrossRef] [PubMed]
12. Diacou, R.; Nandigrami, P.; Fiser, A.; Liu, W.; Ashery-Padan, R.; Cvekl, A. Cell fate decisions, transcription factors and signaling during early retinal development. *Prog. Retin. Eye Res.* **2022**, *91*, 101093. [CrossRef] [PubMed]
13. Holt, C. Cell movements in *Xenopus* eye development. *Nature* **1980**, *287*, 850–852. [CrossRef] [PubMed]
14. Chang, W.S.; Harris, W.A. Sequential genesis and determination of cone and rod photoreceptors in *Xenopus*. *J. Neurobiol.* **1998**, *35*, 227–244. [PubMed]
15. Le Blay, K.; Préau, L.; Morvan-Dubois, G.; Demeneix, B. Expression of the inactivating deiodinase, Deiodinase 3, in the pre-metamorphic tadpole retina. *PLoS ONE* **2018**, *13*, e0195374. [CrossRef]
16. Straznicky, K.; Gaze, R.M. The growth of the retina in *Xenopus laevis*: An autoradiographic study. *Development* **1971**, *26*, 67–79. [CrossRef]
17. Man, L.L.H.; Storey, S.S.; Bertolesi, G.E.; McFarlane, S. Cell-type expression and activation by light of neuropsins in the developing and mature Xenopus retina. *Front. Cell Neurosci.* **2023**, *17*, 1266945. [CrossRef]
18. Liao, Y.; Ma, L.; Guo, Q.; E, W.; Fang, X.; Yang, L.; Ruan, F.; Wang, J.; Zhang, P.; Sun, Z.; et al. Publisher Correction: Cell landscape of larval and adult *Xenopus laevis* at single-cell resolution. *Nat. Commun.* **2022**, *13*, 5142. [CrossRef] [PubMed]
19. Briggs, J.A.; Weinreb, C.; Wagner, D.E.; Megason, S.; Peshkin, L.; Kirschner, M.W.; Klein, A.M. The dynamics of gene expression in vertebrate embryogenesis at single-cell resolution. *Science* **2018**, *360*, eaar5780. [CrossRef]
20. Ding, Y.; Colozza, G.; Zhang, K.; Moriyama, Y.; Ploper, D.; Sosa, E.A.; Benitez, M.D.J.; De Robertis, E.M. Genome-wide analysis of dorsal and ventral transcriptomes of the *Xenopus laevis* gastrula. *Dev. Biol.* **2017**, *426*, 176–187. [CrossRef]
21. Giudetti, G.; Giannaccini, M.; Biasci, D.; Mariotti, S.; Degl'innocenti, A.; Perrotta, M.; Barsacchi, G.; Andreazzoli, M. Characterization of the Rx1-dependent transcriptome during early retinal development. *Dev. Dyn.* **2014**, *243*, 1352–1361. [CrossRef] [PubMed]
22. Viczian, A.S.; Solessio, E.C.; Lyou, Y.; Zuber, M.E. Generation of functional eyes from pluripotent cells. *PLoS Biol.* **2009**, *7*, e1000174. [CrossRef]
23. Casarosa, S.; Amato, M.A.; Andreazzoli, M.; Gestri, G.; Barsacchi, G.; Cremisi, F. Xrx1 controls proliferation and multipotency of retinal progenitors. *Mol. Cell Neurosci.* **2003**, *22*, 25–36. [CrossRef] [PubMed]
24. Louie, S.H.; Fisher, M.; Grainger, R.M. Elucidating the framework for specification and determination of the embryonic retina. *Exp. Cell Res.* **2020**, *397*, 112316. [CrossRef] [PubMed]
25. Bessodes, N.; Parain, K.; Bronchain, O.; Bellefroid, E.J.; Perron, M. Prdm13 forms a feedback loop with Ptf1a and is required for glycinergic amacrine cell genesis in the *Xenopus* Retina. *Neural Dev.* **2017**, *12*, 16. [CrossRef]
26. Parain, K.; Mazurier, N.; Bronchain, O.; Borday, C.; Cabochette, P.; Chesneau, A.; Colozza, G.; El Yakoubi, W.; Hamdache, J.; Locker, M.; et al. A large scale screen for neural stem cell markers in *Xenopus* retina. *Dev. Neurobiol.* **2012**, *72*, 491–506. [CrossRef] [PubMed]
27. Martini, D.; Digregorio, M.; Voto, I.A.P.; Morabito, G.; Degl'Innocenti, A.; Giudetti, G.; Giannaccini, M.; Andreazzoli, M. Kdm7a expression is spatiotemporally regulated in developing *Xenopus laevis* embryos, and its overexpression influences late retinal development. *Dev. Dyn.* **2024**, *253*, 508–518. [CrossRef]
28. Ledford, K.L.; Martinez-De Luna, R.I.; Theisen, M.A.; Rawlins, K.D.; Viczian, A.S.; Zuber, M.E. Distinct cis-acting regions control six6 expression during eye field and optic cup stages of eye formation. *Dev. Biol.* **2017**, *426*, 418–428. [CrossRef]

29. Zaghloul, N.A.; Moody, S.A. Alterations of rx1 and pax6 expression levels at neural plate stages differentially affect the production of retinal cell types and maintenance of retinal stem cell qualities. *Dev. Biol.* **2007**, *306*, 222–240. [CrossRef]
30. Zaghloul, N.A.; Moody, S.A. Changes in Rx1 and Pax6 activity at eye field stages differentially alter the production of amacrine neurotransmitter subtypes in *Xenopus*. *Mol. Vis.* **2007**, *13*, 86–95.
31. Wong, L.L.; Rapaport, D.H. Defining retinal progenitor cell competence in *Xenopus laevis* by clonal analysis. *Development* **2009**, *136*, 1707–1715. [CrossRef]
32. Sive, H.L.; Grainger, R.M.; Harland, R.M. *Early Development of Xenopus laevis: A Laboratory Manual*; Cold Spring Harbor Laboratory Press: Long Island, NY, USA, 2000.
33. Nieuwkoop, P.D.; Faber, J. *Normal Table of Xenopus laevis (Daudin): A Systematical and Chronological Survey of the Development from the Fertilized Egg Till the End of Matamorphosis*; North-Holland Publishing Company: Amsterdam, The Netherlands, 1975.
34. Kha, C.X.; Guerin, D.J.; Tseng, K.A. Studying In Vivo Retinal Progenitor Cell Proliferation in *Xenopus laevis*. *Methods Mol. Biol.* **2020**, *2092*, 19–33. [CrossRef]
35. McDonough, M.J.; Allen, C.E.; Ng-Sui-Hing, N.K.; Rabe, B.A.; Lewis, B.B.; Saha, M.S. Dissection, culture, and analysis of *Xenopus laevis* embryonic retinal tissue. *J. Vis. Exp.* **2012**, *70*, e4377. [CrossRef]
36. Bowes, J.B.; Snyder, K.A.; Segerdell, E.; Jarabek, C.J.; Azam, K.; Zorn, A.M.; Vize, P.D. Xenbase: Gene expression and improved integration. *Nucleic Acids Res.* **2010**, *38*, D607–D612. [CrossRef] [PubMed]
37. Fisher, M.; James-Zorn, C.; Ponferrada, V.; Bell, A.J.; Sundararaj, N.; Segerdell, E.; Chaturvedi, P.; Bayyari, N.; Chu, S.; Pells, T.; et al. Xenbase: Key features and resources of the *Xenopus* model organism knowledgebase. *Genetics* **2023**, *224*, iyad018. [CrossRef] [PubMed]
38. Fisher, M.E.; Segerdell, E.; Matentzoglu, N.; Nenni, M.J.; Fortriede, J.D.; Chu, S.; Pells, T.J.; Osumi-Sutherland, D.; Chaturvedi, P.; James-Zorn, C.; et al. The Xenopus phenotype ontology: Bridging model organism phenotype data to human health and development. *BMC Bioinform.* **2022**, *23*, 99. [CrossRef]
39. Xue, X.Y.; Harris, W.A. Using myc genes to search for stem cells in the ciliary margin of the *Xenopus* retina. *Dev. Neurobiol.* **2012**, *72*, 475–490. [CrossRef]
40. Khosrowshahian, F.; Wolanski, M.; Chang, W.Y.; Fujiki, K.; Jacobs, L.; Crawford, M.J. Lens and retina formation require expression of Pitx3 in *Xenopus* pre-lens ectoderm. *Dev. Dyn.* **2005**, *234*, 577–589. [CrossRef]
41. Furukawa, T.; Morrow, E.M.; Cepko, C.L. Crx, a novel otx-like homeobox gene, shows photoreceptor-specific expression and regulates photoreceptor differentiation. *Cell* **1997**, *91*, 531–541. [CrossRef]
42. Hoshino, A.; Ratnapriya, R.; Brooks, M.J.; Chaitankar, V.; Wilken, M.S.; Zhang, C.; Starostik, M.R.; Gieser, L.; La Torre, A.; Nishio, M.; et al. Molecular Anatomy of the Developing Human Retina. *Dev. Cell* **2017**, *43*, 763–779.e4. [CrossRef]
43. Clark, B.S.; Stein-O'Brien, G.L.; Shiau, F.; Cannon, G.H.; Davis-Marcisak, E.; Sherman, T.; Santiago, C.P.; Hoang, T.V.; Rajaii, F.; James-Esposito, R.E.; et al. Single-Cell RNA-Seq Analysis of Retinal Development Identifies NFI Factors as Regulating Mitotic Exit and Late-Born Cell Specification. *Neuron* **2019**, *102*, 1111–1126.e5. [CrossRef] [PubMed]
44. Muto, A.; Iida, A.; Satoh, S.; Watanabe, S. The group E Sox genes Sox8 and Sox9 are regulated by Notch signaling and are required for Müller glial cell development in mouse retina. *Exp. Eye Res.* **2009**, *89*, 549–558. [CrossRef]
45. Aleksander, S.A.; Balhoff, J.; Carbon, S.; Cherry, J.M.; Drabkin, H.J.; Ebert, D.; Feuermann, M.; Gaudet, P.; Harris, N.L.; Hill, D.P.; et al. The Gene Ontology knowledgebase in 2023. *Genetics* **2023**, *224*, iyad031. [CrossRef]
46. Kha, C.X.; Tseng, K.A. Developmental dependence for functional eye regrowth in *Xenopus laevis*. *Neural Regen. Res.* **2018**, *13*, 1735–1737. [CrossRef]
47. Viczian, A.S.; Zuber, M.E. A simple behavioral assay for testing visual function in *Xenopus laevis*. *J. Vis. Exp.* **2014**, *88*, 51726. [CrossRef]
48. Locker, M.; Agathocleous, M.; Amato, M.A.; Parain, K.; Harris, W.A.; Perron, M. Hedgehog signaling and the retina: Insights into the mechanisms controlling the proliferative properties of neural precursors. *Genes Dev.* **2006**, *20*, 3036–3048. [CrossRef]
49. Agathocleous, M.; Iordanova, I.; Willardsen, M.I.; Xue, X.Y.; Vetter, M.L.; Harris, W.A.; Moore, K.B. A directional Wnt/beta-catenin-Sox2-proneural pathway regulates the transition from proliferation to differentiation in the *Xenopus* retina. *Development* **2009**, *136*, 3289–3299. [CrossRef] [PubMed]
50. Sakagami, K.; Gan, L.; Yang, X.J. Distinct effects of Hedgehog signaling on neuronal fate specification and cell cycle progression in the embryonic mouse retina. *J. Neurosci.* **2009**, *29*, 6932–6944. [CrossRef]
51. Amato, M.A.; Boy, S.; Perron, M. Hedgehog signaling in vertebrate eye development: A growing puzzle. *Cell Mol. Life Sci.* **2004**, *61*, 899–910. [CrossRef] [PubMed]
52. Cavodeassi, F.; Creuzet, S.; Etchevers, H.C. The hedgehog pathway and ocular developmental anomalies. *Hum. Genet.* **2019**, *138*, 917–936. [CrossRef]
53. Fuhrmann, S. Wnt signaling in eye organogenesis. *Organogenesis* **2008**, *4*, 60–67. [CrossRef] [PubMed]
54. Van Raay, T.J.; Moore, K.B.; Iordanova, I.; Steele, M.; Jamrich, M.; Harris, W.A.; Vetter, M.L. Frizzled 5 signaling governs the neural potential of progenitors in the developing *Xenopus* retina. *Neuron* **2005**, *46*, 23–36. [CrossRef] [PubMed]
55. Burns, C.J.; Zhang, J.; Brown, E.C.; Van Bibber, A.M.; Van Es, J.; Clevers, H.; Ishikawa, T.O.; Taketo, M.M.; Vetter, M.L.; Fuhrmann, S. Investigation of Frizzled-5 during embryonic neural development in mouse. *Dev. Dyn.* **2008**, *237*, 1614–1626. [CrossRef]
56. Clevers, H.; Loh, K.M.; Nusse, R. Stem cell signaling. An integral program for tissue renewal and regeneration: Wnt signaling and stem cell control. *Science* **2014**, *346*, 1248012. [CrossRef] [PubMed]

57. Wong-Riley, M.T. Energy metabolism of the visual system. *Eye Brain* **2010**, *2*, 99–116. [CrossRef] [PubMed]
58. Oginuma, M.; Moncuquet, P.; Xiong, F.; Karoly, E.; Chal, J.; Guevorkian, K.; Pourquié, O. A Gradient of Glycolytic Activity Coordinates FGF and Wnt Signaling during Elongation of the Body Axis in Amniote Embryos. *Dev. Cell* **2017**, *40*, 342–353.e10. [CrossRef]
59. Miyazawa, H.; Aulehla, A. Revisiting the role of metabolism during development. *Development* **2018**, *145*, dev131110. [CrossRef]
60. Reddien, P.W. Principles of regeneration revealed by the planarian eye. *Curr. Opin. Cell Biol.* **2021**, *73*, 19–25. [CrossRef]
61. Silva, N.J.; Nagashima, M.; Li, J.; Kakuk-Atkins, L.; Ashrafzadeh, M.; Hyde, D.R.; Hitchcock, P.F. Inflammation and matrix metalloproteinase 9 (Mmp-9) regulate photoreceptor regeneration in adult zebrafish. *Glia* **2020**, *68*, 1445–1465. [CrossRef]
62. Gozlan, O.; Sprinzak, D. Notch signaling in development and homeostasis. *Development* **2023**, *150*, dev201138. [CrossRef]
63. Hori, K.; Sen, A.; Artavanis-Tsakonas, S. Notch signaling at a glance. *J. Cell Sci.* **2013**, *126*, 2135–2140. [CrossRef]
64. Henrique, D.; Schweisguth, F. Mechanisms of Notch signaling: A simple logic deployed in time and space. *Development* **2019**, *146*, dev172148. [CrossRef] [PubMed]
65. Coffman, C.R.; Skoglund, P.; Harris, W.A.; Kintner, C.R. Expression of an extracellular deletion of Xotch diverts cell fate in Xenopus embryos. *Cell* **1993**, *73*, 659–671. [CrossRef] [PubMed]
66. Schneider, M.L.; Turner, D.L.; Vetter, M.L. Notch signaling can inhibit Xath5 function in the neural plate and developing retina. *Mol. Cell Neurosci.* **2001**, *18*, 458–472. [CrossRef]
67. Ohnuma, S.; Philpott, A.; Wang, K.; Holt, C.E.; Harris, W.A. $p27^{Xic1}$, a Cdk inhibitor, promotes the determination of glial cells in *Xenopus* retina. *Cell* **1999**, *99*, 499–510. [CrossRef] [PubMed]
68. Marsh-Armstrong, N.; Huang, H.; Remo, B.F.; Liu, T.T.; Brown, D.D. Asymmetric growth and development of the *Xenopus laevis* retina during metamorphosis is controlled by type III deiodinase. *Neuron* **1999**, *24*, 871–878. [CrossRef]
69. Perron, M.; Kanekar, S.; Vetter, M.L.; Harris, W.A. The genetic sequence of retinal development in the ciliary margin of the *Xenopus* eye. *Dev. Biol.* **1998**, *199*, 185–200. [CrossRef] [PubMed]
70. Zhang, F.; Zhang, J.; Li, X.; Li, B.; Tao, K.; Yue, S. Notch signaling pathway regulates cell cycle in proliferating hepatocytes involved in liver regeneration. *J. Gastroenterol. Hepatol.* **2018**, *33*, 1538–1547. [CrossRef]
71. Zhao, L.; Borikova, A.L.; Ben-Yair, R.; Guner-Ataman, B.; MacRae, C.A.; Lee, R.T.; Burns, C.G.; Burns, C.E. Notch signaling regulates cardiomyocyte proliferation during zebrafish heart regeneration. *Proc. Natl. Acad. Sci. USA* **2014**, *111*, 1403–1408. [CrossRef]
72. Campbell, L.J.; Levendusky, J.L.; Steines, S.A.; Hyde, D.R. Retinal regeneration requires dynamic Notch signaling. *Neural Regen. Res.* **2022**, *17*, 1199–1209. [CrossRef]
73. Kraus, J.M.; Giovannone, D.; Rydzik, R.; Balsbaugh, J.L.; Moss, I.L.; Schwedler, J.L.; Bertrand, J.Y.; Traver, D.; Hankenson, K.D.; Crump, J.G.; et al. Notch signaling enhances bone regeneration in the zebrafish mandible. *Development* **2022**, *149*, dev199995. [CrossRef]
74. Guerin, D.J.; Gutierrez, B.; Zhang, B.; Tseng, K.A.-S. Notch is Required for Neural Progenitor Proliferation during Embryonic Eye Regrowth. *bioRxiv* **2024**. [CrossRef]
75. Raj, B.; Wagner, D.E.; McKenna, A.; Pandey, S.; Klein, A.M.; Shendure, J.; Gagnon, J.A.; Schier, A.F. Simultaneous single-cell profiling of lineages and cell types in the vertebrate brain. *Nat. Biotechnol.* **2018**, *36*, 442–450. [CrossRef] [PubMed]
76. Hu, Y.; Wang, X.; Hu, B.; Mao, Y.; Chen, Y.; Yan, L.; Yong, J.; Dong, J.; Wei, Y.; Wang, W.; et al. Dissecting the transcriptome landscape of the human fetal neural retina and retinal pigment epithelium by single-cell RNA-seq analysis. *PLoS Biol.* **2019**, *17*, e3000365. [CrossRef]
77. Lu, Y.; Shiau, F.; Yi, W.; Lu, S.; Wu, Q.; Pearson, J.D.; Kallman, A.; Zhong, S.; Hoang, T.; Zuo, Z.; et al. Single-Cell Analysis of Human Retina Identifies Evolutionarily Conserved and Species-Specific Mechanisms Controlling Development. *Dev. Cell* **2020**, *53*, 473–491.e9. [CrossRef] [PubMed]
78. Session, A.M.; Uno, Y.; Kwon, T.; Chapman, J.A.; Toyoda, A.; Takahashi, S.; Fukui, A.; Hikosaka, A.; Suzuki, A.; Kondo, M.; et al. Genome evolution in the allotetraploid frog *Xenopus laevis*. *Nature* **2016**, *538*, 336–343. [CrossRef]
79. Elurbe, D.M.; Paranjpe, S.S.; Georgiou, G.; van Kruijsbergen, I.; Bogdanovic, O.; Gibeaux, R.; Heald, R.; Lister, R.; Huynen, M.A.; van Heeringen, S.J.; et al. Regulatory remodeling in the allo-tetraploid frog *Xenopus laevis*. *Genome Biol.* **2017**, *18*, 198. [CrossRef]
80. Watanabe, M.; Yasuoka, Y.; Mawaribuchi, S.; Kuretani, A.; Ito, M.; Kondo, M.; Ochi, H.; Ogino, H.; Fukui, A.; Taira, M.; et al. Conservatism and variability of gene expression profiles among homeologous transcription factors in *Xenopus laevis*. *Dev. Biol.* **2017**, *426*, 301–324. [CrossRef]
81. Michiue, T.; Yamamoto, T.; Yasuoka, Y.; Goto, T.; Ikeda, T.; Nagura, K.; Nakayama, T.; Taira, M.; Kinoshita, T. High variability of expression profiles of homeologous genes for Wnt, Hh, Notch, and Hippo signaling pathways in *Xenopus laevis*. *Dev. Biol.* **2017**, *426*, 270–290. [CrossRef]
82. Gout, J.F.; Kahn, D.; Duret, L. The relationship among gene expression, the evolution of gene dosage, and the rate of protein evolution. *PLoS Genet.* **2010**, *6*, e1000944. [CrossRef]
83. Aury, J.M.; Jaillon, O.; Duret, L.; Noel, B.; Jubin, C.; Porcel, B.M.; Ségurens, B.; Daubin, V.; Anthouard, V.; Aiach, N.; et al. Global trends of whole-genome duplications revealed by the ciliate *Paramecium tetraurelia*. *Nature* **2006**, *444*, 171–178. [CrossRef] [PubMed]
84. Mears, A.J.; Kondo, M.; Swain, P.K.; Takada, Y.; Bush, R.A.; Saunders, T.L.; Sieving, P.A.; Swaroop, A. Nrl is required for rod photoreceptor development. *Nat. Genet.* **2001**, *29*, 447–452. [CrossRef]

85. Showell, C.; Christine, K.S.; Mandel, E.M.; Conlon, F.L. Developmental expression patterns of Tbx1, Tbx2, Tbx5, and Tbx20 in *Xenopus tropicalis*. *Dev. Dyn.* **2006**, *235*, 1623–1630. [CrossRef] [PubMed]
86. Lee, S.Y.; Yoon, J.; Lee, M.H.; Jung, S.K.; Kim, D.J.; Bode, A.M.; Kim, J.; Dong, Z. The role of heterodimeric AP-1 protein comprised of JunD and c-Fos proteins in hematopoiesis. *J. Biol. Chem.* **2012**, *287*, 31342–31348. [CrossRef] [PubMed]
87. Rogers, C.D.; Harafuji, N.; Archer, T.; Cunningham, D.D.; Casey, E.S. *Xenopus* Sox3 activates sox2 and geminin and indirectly represses Xvent2 expression to induce neural progenitor formation at the expense of non-neural ectodermal derivatives. *Mech. Dev.* **2009**, *126*, 42–55. [CrossRef] [PubMed]
88. Yang, J.; Zhu, Y.; Gu, F.; He, X.; Cao, Z.; Li, X.; Tong, Y.; Ma, X. A novel nonsense mutation in CRYBB1 associated with autosomal dominant congenital cataract. *Mol. Vis.* **2008**, *14*, 727–731.